6-2009

Entanglement Perturbation Theory for Antiferromagnetic Spin Chains

Lihua Wang
Western Michigan University

ENTANGLEMENT PERTURBATION THEORY FOR ANTIFERROMAGNETIC SPIN CHAINS

by

Lihua Wang

A Dissertation
Submitted to the
Faculty of The Graduate College
in partial fulfillmen of the
requirements for the
Degree of Doctor of Philosophy
Department of Physics
Advisor: Sung G. Chung, Ph.D.

Western Michigan University
Kalamazoo, Michigan
June 2009

ENTANGLEMENT PERTURBATION THEORY FOR ANTIFERROMAGNETIC SPIN CHAINS

Lihua Wang, Ph.D.

Western Michigan University, 2009

In this dissertation, we use the recently developed Entanglement Perturbation Theory (EPT) to solve antiferromagnetic spin chain problems, for both spin 1/2 and spin 1. We firs use EPT-g (EPT algorithm for ground state) to get the ground state properties. We calculated precisely energies, magnetization and spin-spin correlations. The precision of the long range spin-spin correlation functions for spin 1/2 chains is unprecedented. Due to its special structure, we also use EPT-g to calculate the firs excited state properties for spin 1 chains. Hence we plotted the phase diagram for spin 1 xxz chains. Also a generalization of EPT (EPT-e) for elementary excitation in one dimension determined the spin-triplet magnon spectrum for spin 1 chain for the firs time for the entire Brillouin zone, including the Haldane gap at $k = \pi$. The spin chains, the 2D&3D Ising models, the 1D&2D Hubbard models and the Bose-Hubbard model whose study by EPT is recently started represent a variety of strongly correlated many body systems with translational symmetry. Namely EPT is a general method for them. On the other hand, the successful application of EPT-e indicates EPT's potential to study the inhomogeneous quantum systems.

ACKNOWLEDGMENTS

I would like to gratefully acknowledge the supervision of the committee members. They are Dr. Sung G. Chung, my Ph.D. advisor, Dr. Dean Halderson, Dr. Thomas Gorczyca, Dr. Arthur McGurn and Dr. Yirong Mo from chemistry department. I also want to acknowledge the help with Latex from my colleagues, Mr. Hasoglu Fatih and Mrs. Huaizhen Zhang. This work is partially done on the College of Sciences and Humanities Cluster at Ball State University.

Lihua Wang

TABLE OF CONTENTS

LIST OF TABLES

LIST OF FIGURES

CHAPTER 1

INTRODUCTION

Since the Entanglement Perturbation Theory (EPT) has been successfully applied to typical classical statistical systems, 3D&3D Ising models [22], and typical quantum systems, 1D&2D Hubbard models [23, 24], it is naturally asked if it can be applied to other systems. More precisely, we ask if EPT is a generally effective method for macroscopic quantum systems with translational symmetry. The Heisenburg spin chain an ideal model for this purpose, as it is simple enough yet adequate to represent broad quantum systems. Here we extend the EPT to evaluate both the ground state and the firs excited state properties of the spin chains, while only the ground state properties have been studied in [23, 24].

1.1 Heisenberg spin chains

Despite the simple form of its Hamiltonian, the Heisenberg spin chain has fascinated physicists for generations. Many physicist contributed to its understanding. There are both rigorous solutions like Bethe Ansatz solutions [13, 14, 15, 3, 4, 5] and numerical simulations like Density Matrix Renormalization Group (DMRG)[29, 28, 30], Monte Carlo method [12, 17] and the semi-classical quantum theory due to P. W. Anderson [20]. Even recently workers are still extending the applications to spin chains with impurities [19], the spin-1-spin-1/2 chain [26] and the spin chain with anisotropic coupling strength in x, y, z directions [10]. However, our discussion is mostly restricted to the most fundamental isotropic antiferromagnetic spin chains in this work. Extension to other circumstances is

natural for EPT after the successful application to this model. For example, the phase diagram for spin 1 xxz chains is achieved as well, whose extension from the EPT calculation for isotropic spin chains is simple. We start below with the case of spin 1/2 chains. Later in the chapter 2 we will see that working out the spin-1 Heisenberg spin chain by EPT is straightforward from the spin-1/2 case.

We firs give the Hamiltonian of the spin chain and then briefl review existing works, namely Bethe Ansatz, renormalization group simulation and semi-classical quantum theory. We want to discuss that these methods both share some ideas, and differ in some other aspects. In the following chapters, we will see that EPT also inherits some important concepts from the existing methods like the spin wave structure of the excitation operator on the ground state, and EPT bears some new ideas. For example, it makes most thorough use of the translational symmetry to construct the trial wave function. Now let us look at the Hamiltonian of the antiferromagnetic spin chain

$$H = J\sum_{i=1}^{L}\left(S_i^x \cdot S_{i+1}^x + S_i^y \cdot S_{i+1}^y + S_i^z \cdot S_{i+1}^z\right) \tag{1.1}$$

where J is the coupling strength between the nearest sites, positive for antiferromagnetic spin chain, otherwise for ferromagnetic spin chain. Since the spin z-component of σ on each site has two possible states, $|\uparrow\rangle$ for up spin or $|\downarrow\rangle$ for down spin, the basis vectors span a 2^L dimensional Hilbert space $|\ \sigma_1\sigma_2\cdots\sigma_L\rangle$, if the spin chain length is L.

From now on we use the following form of the Hamiltonian

$$H = J\sum_{i=1}^{L}\left[\frac{1}{2}\left(S_i^+ \cdot S_{i+1}^- + S_i^- \cdot S_{i+1}^+\right) + S_i^z \cdot S_{i+1}^z\right] \tag{1.2}$$

The rules governing operators on the basis vectors are illustrated in the following table

	$\vert\cdots\uparrow\cdots\rangle$	$\vert\cdots\downarrow\cdots\rangle$
S_i^+	$\vert\cdots 0\cdots\rangle$	$\vert\cdots\uparrow\cdots\rangle$
S_i^-	$\vert\cdots\downarrow\cdots\rangle$	$\vert\cdots 0\cdots\rangle$
S_i^z	$\frac{1}{2}\vert\cdots\uparrow\cdots\rangle$	$-\frac{1}{2}\vert\cdots\downarrow\cdots\rangle$

Table 1.1 Rules governing operators on the basis vectors

There are two important symmetries. The firs one is the translational symmetry. This property implies the spin wave structure of the wave function, as Bloch-Floquet theorem indicates. EPT makes full use of the translational symmetry to introduce periodic structure for both the operator and the local wave function. The second symmetry is the rotational symmetry about one specifi axis, for instance, z-axis. It is, $S_T^z \equiv \sum_{i=1}^{L} S_i^z$ is conserved. Therefore the Hilbert space is divided into subspaces. The total spin z-component is the same for the wave vectors in the same subspace, but different for different subspaces. For the ferromagnetic spin chain, the ground state has the maximum total spin z-component and the lowest excited state emerges when one magnon is excited, while the ground state has zero total spin z-component for the antiferromagnetic spin chain, and shooting in spinons can excite the spin chain from the ground state to low-lying excited states.

1.2 Existing methods

There are some methods for the solution of the spin chains. Among them, Bethe Ansatz [13, 14, 15] gives the rigorous results. As mentioned above, the ground state has to be the one with zero total spin z-component. So the ground state is the superposition of those which have r specifi sites spin up and r other sites spin down, $r = \frac{1}{2}L$, L is the length of the chain. For convenience, we assume L is an even integer from now on. The general

form of the ground state wave function is as follows

$$\mid \psi\rangle = \sum_{1\leq i_1<i_2<\cdots<i_r\leq L} a\left(i_1,\cdots,i_r\right) \mid n_1,\cdots,n_r\rangle \tag{1.3}$$

where $\mid n_1,\cdots,n_r\rangle$ stands for the vector for which site $\{n_1,\cdots,n_r\}$ have z-component spin up, and

$$a\left(i_1,\cdots,i_r\right) = \sum_{\mathcal{P}\in S_r} \exp\left(i\sum_{j=1}^{r} K_{\mathcal{P}_j} n_j + \frac{i}{2}\sum_{j<m}\theta_{\mathcal{P}_j\mathcal{P}_m}\right) \tag{1.4}$$

The sum $\mathcal{P}\in S_r$ is over all $r!$ permutations of the labels $\{1,2,\ldots,r\}$. The phase angles θ_{ij} and the momenta K_i have to satisfy the following Bethe Ansatz equations

$$2cot\frac{\theta_{ij}}{2} = cot\frac{K_i}{2} - cot\frac{K_j}{2}, \qquad \text{i,j=1, . . . ,r} \tag{1.5}$$

$$LK_i = 2\pi\lambda_i + \sum_{j\neq i}\theta_{ij}, \qquad \text{i=1, . . . ,r} \tag{1.6}$$

where

$$\lambda_i \in \{0,1,\ldots,N-1\} \tag{1.7}$$

is the so called Bethe quantum number. What remains to be done is to fin those sets of Bethe quantum numbers $\{\lambda_1,\lambda_2,\ldots,\lambda_r\}$ which yield solutions of the Bethe Ansatz equations (1.5) and (1.6). Notice that those solutions might be real or complex. Every solution represents an eigenvector with energy

$$E - E_0 = J\sum_{j=1}^{r}(1-\cos K_j) \tag{1.8}$$

with E_0 being the energy for all sites z-component spin up state. The wave number is define by

$$K = \frac{2\pi}{L}\sum_{i=1}^{r}\lambda_i \tag{1.9}$$

Figure 1.1 Configurations of Bethe quantum numbers for $L = 32$ ground state (top row) and for one representative of three sets of two-spinon excitations.

Without going into too many details, we directly write out the ground state for antiferromagnetic spin-1/2 Heisenberg spin chain as follows

$$\mid A\rangle : \{\lambda_i\}_A = \{1, 3, 5, \ldots, L-1\} \tag{1.10}$$

If we think the ground state $\mid A\rangle$ as the reference state for all excited states, the Bethe quantum number (1.7) is represented by a perfectly regular array on the integer axis as illustrated in the firs row of Fig.1.1. This array will be interpreted as a physical vacuum. The low-lying excited states emerge when spinons are shot into this vacuum. As seen in Fig.1.1, the two-spinon excitations can be sorted into triplet states with $S_T = 1, S_T^z = 0, \pm 1$ and the other singlets, $S_T = 0$. It is because unlike magnons, which are spin-1 particles, spinons are spin-1/2 particles. In a chain with even L, where all eigenstates have integer-valued S_T^z, spinons occur only in pairs. The spin $S_l = \pm\frac{1}{2}, l = 1, 2$ of the two spinons in

a two-spinon eigenstate of Hamiltonian can be combined in four different ways to form a triplet state or a singlet state, they are described by distinct configuratio of Bethe quantum numbers. In Fig.1.1 rows two to four are three sets of two-spinon excitations with energy $E_q^{S_T,S_T^z}$. Each gap in the integer array of rows two and three (green full circles) represents a spinon. Each gap in row four (green open circles) represents half a spinon. Actually in the Bethe quantum number configuratio of row four, they are no more all real numbers. Instead, the blue circle on row four represents the Bethe quantum number associated with a pair of complex conjugate solutions. While, all black circles in Fig.1.1 are associated with real solutions.

Even though the two-spinon singlets play an important role in the zero-temperature spin dynamics of quasi-1D antiferromagnetic compounds[14], they cannot be excited directly from the ground state by neutrons because of selection rules. Hence we only talk about the two-spinon excitation with real Bethe quantum numbers, associated by the wave numbers K_1, K_2, which in turn add up to the wave number of the two-spinon state relative to the wave number of the ground state:

$$q \equiv K1 + K2 \tag{1.11}$$

After definin the wave number of the low-lying excited state, one can calculate the dispersion relation. We fin from Bethe Ansatz that the excitation energy varies continuously from the ground state with the wave number for infinit antiferromagnetic Heisenberg spin-1/2 chain. In contrast, there is a finit gap in the energy from ground sate to the lowest excited state for integer-spin antiferromagnetic chains, the so called Haldane gap [7]. One

of the tasks of our work is to capture this phenomenon by EPT calculation.

Besides the Bethe Ansatz rigorous solutions, P. W. Anderson's spin wave theory of the antiferromagnetic ground state[20] is semi-classical, but carries physically meaningful idea. The basic assumption in deriving the semi-classical spin waves is that the state of the antiferromagnetic spin chain is not greatly different from the calssical ground state in which the spins of the one sublattice (either even sites or odd sites) all point to positive z-direction while the rest all in the other direction. Mathematically, it can be written as

$$S_i^z \approx +S \tag{1.12}$$

$$S_{i+1}^z \approx -S \tag{1.13}$$

$$\tag{1.14}$$

If we introduce S_c as the classical total spin of an atom with spin quantum number S, we can write the Hamiltonian only in term of the two spin components S_x and S_y

$$(S_z)^2 = S_c^2 - \left((S^x)^2 + (S^y)^2\right) \tag{1.15}$$

$$S_c = [S(S+1)]^{1/2} \tag{1.16}$$

Write $S_{i,i+1}^{x,y}$ in spinwave form of the Fourier counterpart $Q_{i,i+1}^{x,y}$, the Hamiltonian can be written in the quadratic form by a canonical transformation, which can be readily solved.

Finally, there are some numerical simulations, among which the density matrix renormalization group (DMRG) method achieves great accuracy[29, 28]. Always working in a much smaller subspace by truncating the Hilbert space according to the density matrix, one can calculate larger and larger spin chains. However, obviously one can not go for a truly

infinit spin chain this way. Since EPT does not need this Hilbert space truncation, it can go beyond this limitation, which will be discussed in the following chapters.

CHAPTER 2

EPT FOR THE GROUND STATE

2.1 Overview

EPT fully makes use of the translational symmetry of the system. First EPT introduces the local trial wave functions and then couples them by entanglement to describe the translationally symmetric wave function. Second it reaches a general yet simple algebraic procedure to solve the local trial wave function, during which EPT will utilize the translational symmetry of the Hamiltonian to greatly simplify the formulation. In the second step, we have different ways to handle the operator, i.e., we either deal with the Halmiltonian itself or the density matrix, $e^{-\beta H}$. In fact, at the beginning of EPT development it was $e^{-\beta H}$ that was handled for the 2D&3D Ising models. This algorithm was given the name EPT-g1. Later EPT-g2 algorithm was developed to handle the Hamiltonian directly. Generally speaking, EPT-g2 formulation is more lengthy. We will discuss EPT-g1 in the following Sec.2.2 and then EPT-g2 in Sec.2.3. The comparison between them is given in Sec.2.4. However we firs talk about how to introduce the local trial wave functions below, as this step is common to both EPT-g1 and EPT-g2.

We take a four-sites spin chain as an example to illustrate how to write the wave function in the product of local trial wave functions. The number of local spin states is denoted as z. So z is 2 for spin 1/2 and 3 for spin 1. The wave function of this spin chain is written as $\psi(a_1, a_2, a_3, a_4)$, which is a z^4 dimensional vector. However it can also be regarded as a z by z^3 matrix $\psi(a_1, a_2a_3a_4)$. We then use singular value decomposition (SVD) to rewrite it

as

$$\psi\left(a_1, a_2 a_3 a_4\right) = A_{a_1,a}\lambda_a B_{a_2 a_3 a_4,a} \tag{2.1}$$

$$= A'_{a_1,a} B_{a_2 a_3 a_4,a} \tag{2.2}$$

Where the eigenvalue λ_a of ψ is absorbed into $A_{a_1,a}$ to give $A'_{a_1,a}$. We then SVD $B_{a_2 a_3 a_4,a}$ to separate a_2 from $a_3 a_4$, we have

$$B_{a_2 a_3 a_4,a} = C_{a_2,ab}\eta_b D_{a_3 a_4,b} \tag{2.3}$$

$$= C'_{a_2,ab} D_{a_3 a_4,b} \tag{2.4}$$

We keep using SVD until all lattice sites are separated from each other and the eigenvalues are properly absorbed into the corresponding left matrices, which can now be regarded as wave functions or vectors of local states $a_1 a_2 a_3 a_4$. Finally the wave function ends up as

$$\psi\left(a_1, a_2, a_3, a_4\right) = A'_{a_1,a} C'_{a_2,ab} E'_{a_3,bc} F_{a_4,c} \tag{2.5}$$

The above shows how to use SVD to rewrite the wave function as a successive product of local ones. We borrow the terminology 'entanglement' from quantum information theory to denote the coupling indices *abcd* in equation (2.5). Now recall that the spin chain is translationally symmetric and has a periodic boundary condition. We should also introduce some uniform local trial wave function ξ to represent the local vectors $A'C'E'F$. Considering the possible $\uparrow\downarrow$ or $\downarrow\uparrow$ spin arrangement for antiferromagnetic spin chains, we need two local trial wave functions ξ^1 and ξ^2 to include such bi-site structure. Therefore we have

the SVD-ed wave function for a general spin chain as follows

$$\psi = \cdots \xi^2_{aba_1} \bigotimes \xi^1_{bca_2} \bigotimes \xi^2_{cda_3} \bigotimes \xi^1_{dea_4} \cdots \tag{2.6}$$

As one might complain that there are too many indices involved above, let us now briefl clarify them. The subscript of 1 on the shoulder refers to the odd site of the chain while 2 the even site. The indices $\{a, b, c, d, e\}$ are the entanglement indices, which are integers, uniformly coupling the local trial wave functions over all spin sites. The larger entanglement will give more precise representation of the net wave function by local trial wave functions. If it is large enough, the wave function could be exactly rebuilt. However, the previous case studies by EPT and the spin chain calculations in this work all show that one can get convergence with entanglement rather quickly. Therefore EPT calculation has very high efficien y. The rest sort of indices above, $\{a_1, a_2, a_3, a_4\}$, account for the local spin state, running from 1 to 2 for spin 1/2, 1 to 3 for spin 1. We use the Fig.2.1 to end up this section, which visually illustrates how the wave function is expressed in term of the local trial wave functions.

2.2 EPT-g1

Since any eigenstate $\mid \psi_i\rangle$ of H is also the eigenstate of density matrix $e^{-\beta H}$, the ground state now bears the largest eigenvalue $e^{-\beta E_0}$. The eigenvalue problem we try to solve is as follows

$$e^{-\beta H} \mid \psi_i\rangle = e^{-\beta E_i} \mid \psi_i\rangle \tag{2.7}$$

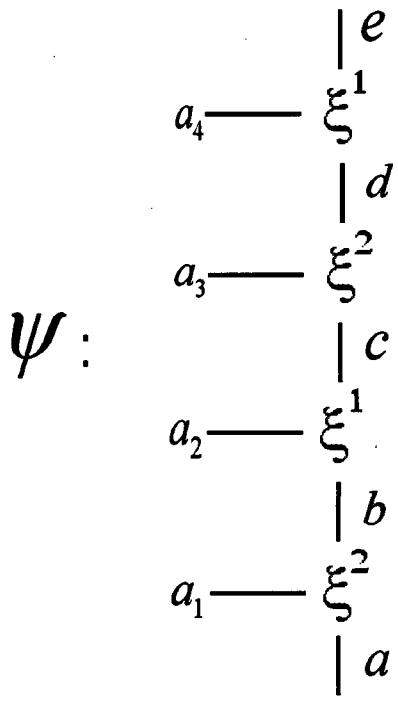

Figure 2.1 Schematic figure of the wave function

We write the Hamiltonian as the sum of the local bond operators between two nearest neighbors

$$H = \sum_{bond} H_{bond} \tag{2.8}$$

with

$$H_{bond} \equiv \frac{j}{2}\left(S_i^+ S_{i+1}^- + S_i^- S_{i+1}^+\right) + j S_i^z S_{i+1}^z \tag{2.9}$$

We then choose appropriate small positive β ($0 < \beta \ll 1$) to safely separate the even and odd sublattices in the density matrix

$$e^{-\beta H} = \prod_{bond} e^{-\beta H_{bond}} + \mathcal{O}\left(\beta^2\right) \approx e^{-\beta \sum_{even} H_{bond}} e^{-\beta \sum_{odd} H_{bond}} \tag{2.10}$$

Now let us linearize $e^{-\beta H_{bond}}$, again, due to the fact that $0 < \beta \ll 1$

$$\begin{aligned} e^{-\beta H_{bond}} &\approx 1 - \frac{j\beta}{2}\left(S_i^+ S_{i+1}^- + S_i^- S_{i+1}^+\right) - j\beta S_i^z S_{i+1}^z \\ &\equiv \Omega_\alpha \bigotimes \Theta_\alpha \end{aligned}$$

where Ω_α takes four operators $1, S_i^+, S_i^-, S_i^z$ on site i and Θ_α likewise operators on site $i+1$. So index α runs from 1 to 4. The local density matrix can be written as

$$\langle lk \mid e^{-\beta H_{bond}} \mid ij \rangle \approx f_{\alpha,ik} \bigotimes g_{\alpha,jl} \tag{2.11}$$

where, for a spin 1/2 chain,

$$f_1 = g_1 = \begin{pmatrix} 1 & 0 \\ 0 & 1 \end{pmatrix} \tag{2.12}$$

$$f_2 = i\sqrt{\frac{\beta J}{2}} \begin{pmatrix} 0 & 1 \\ 0 & 0 \end{pmatrix} \tag{2.13}$$

$$g_2 = i\sqrt{\frac{\beta J}{2}} \begin{pmatrix} 0 & 0 \\ 1 & 0 \end{pmatrix} \tag{2.14}$$

and so on. For a spin 1 chain, f's and g's should be 3 by 3 matrices.

Now let us write down the matrix representation of the even and odd bonds in the density matrix as follows

$$\cdots f_\alpha \bigotimes g_\alpha \bigotimes f_\gamma \bigotimes g_\gamma \cdots$$

$$\cdots f_\beta \bigotimes g_\beta \bigotimes f_\delta \bigotimes g_\delta \cdots$$

The vertical alignment in the above means the matrix representations are at the same spin site. The whole density matrix will be written as

$$\begin{aligned} K &\equiv \cdots g_\alpha \cdot f_\beta \bigotimes f_\gamma \cdot g_\beta \cdots \\ &\equiv \cdots \Gamma^2_{\alpha\beta} \bigotimes \Gamma^1_{\beta\gamma} \cdots \end{aligned} \tag{2.15}$$

Fig.2.2 illustrates the density matrix eigenvalue problem

$$\begin{aligned} K\psi &= e^{-\beta E}\psi \\ &\equiv \mu\psi \end{aligned} \tag{2.16}$$

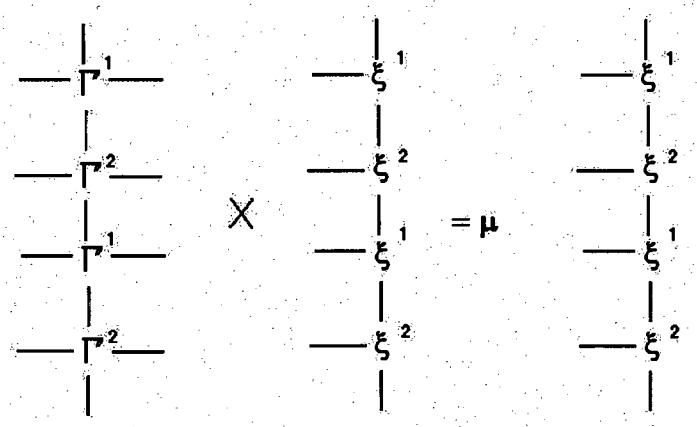

Figure 2.2 Schematic figure of the density matrix eigenvalue equation

The density matrix eigenvalue problem is equivalent to the variational problem where we vary the following quantity with respect to the trial wave function ψ and hence ξ^1 and ξ^2,

$$\delta\left(\frac{\langle\psi \mid K \mid \psi\rangle}{\langle\psi \mid \psi\rangle}\right) = 0 \tag{2.17}$$

where

$$\langle\psi \mid K \mid \psi\rangle = Tr\left(A^{L/2}\right) \tag{2.18}$$

$$\langle\psi \mid \psi\rangle = Tr\left(B^{L/2}\right) \tag{2.19}$$

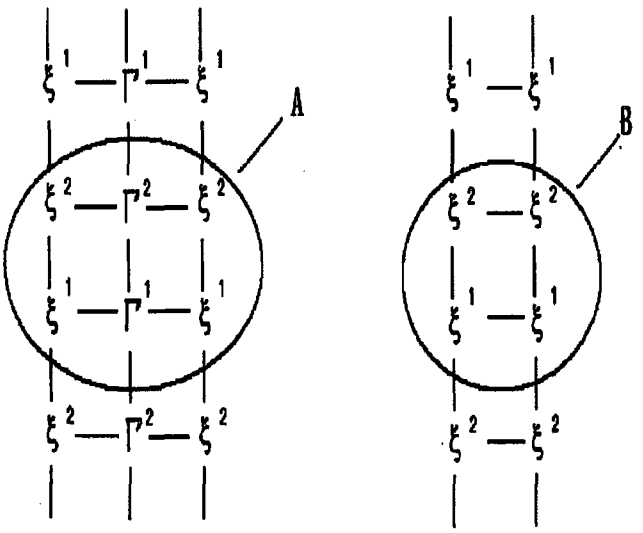

Figure 2.3 Schematic figure of the ground state energy calculation

and

$$A_{m_1,n_1} = \sum_{a_1,a_2,b_1,b_2=1}^{z} \sum_{e,f=1}^{p} \sum_{\beta=1}^{4} \xi^1_{aea_1} \xi^2_{eca_2} \xi^1_{bfb_1} \xi^2_{fdb_2} \Gamma^1_{\alpha\beta,a_1a_2} \Gamma^2_{\beta\gamma,b_1b_2} \tag{2.20}$$

$$B_{m,n} = \sum_{a_1,a_2=1}^{z} \sum_{e,f=1}^{p} \xi^1_{aea_1} \xi^2_{eca_2} \xi^1_{bfa_1} \xi^2_{fda_2} \tag{2.21}$$

$$m_1 = (\gamma - 1) \times p^2 + (b - 1) \times p + a$$

$$n_1 = (\alpha - 1) \times p^2 + (d - 1) \times p + c$$

$$m = (b - 1) \times p + a$$

$$n = (d - 1) \times p + c$$

Fig.2.2 illustrates the structure of the above matrices A and B. The variation (2.17)

leads to

$$A^{L/2-1} * (\delta A) = \mu B^{L/2-1} * (\delta B) \tag{2.22}$$

The definitio of the operation $*$ between two matrices is as follows

$$A * B = \sum_i \sum_j A_{ij} B_{ji} \tag{2.23}$$

We then diagonalize the matrices A and B:

$$A = R \Lambda L \tag{2.24}$$

$$B = R' \Lambda' L' \tag{2.25}$$

Equation (2.17) is further rewritten as follows

$$\sum_{i=1}^{4p^2} (\Lambda_i)^{L/2-1} L_i (\delta A) R_i = \mu \sum_{i=1}^{p^2} (\Lambda'_i)^{L/2-1} L'_i (\delta B) R'_i \tag{2.26}$$

Now we can explicitly work out the variation with respect to the trial local wave functions, for example, ξ^1. Using equation (2.20), (2.26) leads to a generalized eigenvalue equation

$$X_1(aea_1, bfa_2)\xi^1_{bfa_2} = \mu Y_1(aea_1, bfa_2)\xi^1_{bfa_2} \tag{2.27}$$

where

$$X_1(aea_1, bfa_2) = \sum_{i=1}^{4p^2} \sum_{\alpha\beta,\gamma=1}^{4} \sum_{a_3,a_4=1}^{z} \sum_{c,d=1}^{p} \xi^2_{eca_3} \xi^2_{fda_4} \Gamma^1_{\alpha\beta,a_1a_2} \Gamma^2_{\beta\gamma,a_3a_4} R_{cd\gamma,i} L_{ab\alpha,i} (\Lambda_i)^{L/2-1} \tag{2.28}$$

$$Y_1(aea_1, bfa_2) = \sum_{i=1}^{p^2} \sum_{a_3=1}^{z} \sum_{c,d=1}^{p} \xi^2_{eca_3} \xi^2_{fda_3} R'_{cd,i} L'_{ab,i} (\Lambda'_i)^{L/2-1} \delta_{a_1a_2} \tag{2.29}$$

Likewise, we get the generalized eigenvalue equation for ξ^2

$$X_2\xi^2 = \mu Y_2 \xi^2 \tag{2.30}$$

From above, we see that if we choose two arbitrary trial wave functiond ξ_0^1 and ξ_0^2 as the seeds, they will determine two generalized eigenvalue equations

$$X_1\left(\xi_0^1, \xi_0^2\right)\xi^1 = \mu Y_1\left(\xi_0^1, \xi_0^2\right)\xi^1 \tag{2.31}$$

$$X_2\left(\xi_0^1, \xi_0^2\right)\xi^2 = \mu Y_2\left(\xi_0^1, \xi_0^2\right)\xi^2 \tag{2.32}$$

We solve for the next ξ^1 and ξ^2 until convergence. If we keep looking for the largest eigenvalue and corresponding eigenvector, it will arrive at the ground state energy and the local ground state wave function. Otherwise, looking for the second largest will bring about the firs excited state energy and the corresponding wave function.

2.3 EPT-g2

As mentioned in the last section, EPT-g2 handles the Hamiltonian directly. The ground state energy and firs excited state energy can be solved by looking for the firs and second minimum of the quantity

$$\epsilon \equiv \frac{\langle\psi \mid H \mid \psi\rangle}{\langle\psi \mid \psi\rangle} \tag{2.33}$$

Now since both the wave function and the Hamiltonian are translationally symmetric, we rewrite (2.33) as follows

$$\epsilon = \frac{L}{2}\frac{\langle\psi \mid H_{bond}^{odd} \mid \psi\rangle}{\langle\psi \mid \psi\rangle} + \frac{L}{2}\frac{\langle\psi \mid H_{bond}^{even} \mid \psi\rangle}{\langle\psi \mid \psi\rangle} \tag{2.34}$$

where L is the size of the chain and H_{bond} has the same definitio as (2.9). It has the standard matrix representation

$$\Gamma_{b_1 b_2, a_1 a_2} = \langle b_1 \mid \langle b_2 \mid H_{bond} \mid a_1\rangle \mid a_2\rangle \tag{2.35}$$

where $\mid a_1\rangle$ and $\mid a_2\rangle$ refer to the local basis vectors on two neighboring sites while $\langle b_1 \mid$ and $\langle b_2 \mid$ are the conjugate counter parts. Now we are allowed to write (2.34) further as follows

$$\epsilon = \frac{L}{2}\frac{Tr(A^{L/2-1}B)}{Tr(A^{L/2})} + \frac{L}{2}\frac{Tr(C^{L/2-1}D)}{Tr(A^{L/2})} \tag{2.36}$$

where

$$A_{m,n} = \sum_{a_1,a_2=1}^{z}\sum_{e,f=1}^{p} \xi^1_{aea_1}\xi^2_{eca_2}\xi^1_{bfa_1}\xi^2_{fda_2} \tag{2.37}$$

$$B_{m,n} = \sum_{a_1,a_2,b_1,b_2=1}^{z}\sum_{e,f=1}^{p} \xi^1_{aea_1}\xi^2_{eca_2}\xi^1_{bfb_1}\xi^2_{fdb_2}\Gamma_{b_1b_2,a_1a_2} \tag{2.38}$$

$$m = (b-1)\times p + a$$

$$n = (d-1)\times p + c$$

We repeat here that p is the entanglement and z is 2 for spin 1/2, 3 for spin 1. We can write down the matrix of C and D likewise. Fig.2.3 Schematically shows the formation of matrixes A, B, C and D.

If we vary (2.36) with respect to ξ^1 and ξ^2, we will arrive at

$$\begin{aligned}\epsilon A^{L/2-1}(\delta A) = &(\delta B)A^{L/2-1} + \sum_{j=1}^{L/2-1} BA^{L/2-j-1}(\delta A)A^{j-1} \\ &+ (\delta D)C^{L/2-1} + \sum_{j=1}^{L/2-1} DC^{L/2-j-1}(\delta C)C^{j-1}\end{aligned} \tag{2.39}$$

We then diagonalize the matrices A and C:

$$A = R\Lambda L \tag{2.40}$$

$$C = R'\Lambda' L' \tag{2.41}$$

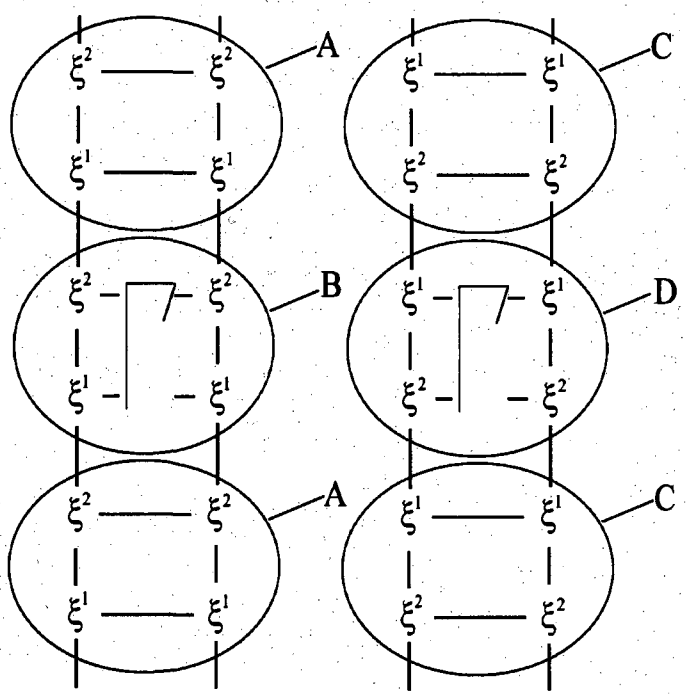

Figure 2.4 Schematic figure of the formation of matrixes A, B, C and D

Equation (2.39) is rewritten as follows

$$\begin{aligned}
&\epsilon \sum_{i=1}^{P^2} (\Lambda_i)^{L/2-1} L_i (\delta A) R_i \\
&= \sum_{i=1}^{P^2} L_i (\Lambda_i)^{L/2-1} (\delta B) R_i + \sum_{i=1}^{P^2} L'_i (\Lambda'_i)^{L/2-1} (\delta D) R'_i + f_1 (L, R, \Lambda, \delta A) + f_2 (L', R', \Lambda', \delta C)
\end{aligned} \tag{2.42}$$

where

$$f_1 (L, R, \Lambda, \delta A) = \left(\sum_{m,n=1;m\neq n}^{P^2} \frac{\Lambda_m^{L/2-1} - \Lambda_n^{L/2-1}}{\Lambda_m - \Lambda_n} + \sum_{m=1}^{P^2} \Lambda_m^{L/2-2} \right) E_{mn} L_n (\delta A) R_m$$

$$f_2 (L', R', \Lambda', \delta C) = \left(\sum_{m,n=1;m\neq n}^{P^2} \frac{(\Lambda'_m)^{L/2-1} - (\Lambda'_n)^{L/2-1}}{\Lambda'_m - \Lambda'_n} + \sum_{m=1}^{P^2} (\Lambda'_m)^{L/2-2} \right) F_{mn} L'_n (\delta C) R'_m$$

$$E_{mn} = L_m B R_n$$

$$F_{mn} = L'_m D R'_n$$

Like what we did for EPT-g1, we choose two arbitrary trial wave functions ξ_0^1 and ξ_0^2 as the seeds and solve the following two generalized eigenvalue equations

$$X_1 \left(\xi_0^1, \xi_0^2\right) \xi^1 = \epsilon Y_1 \left(\xi_0^1, \xi_0^2\right) \xi^1 \tag{2.43}$$

$$X_2 \left(\xi_0^1, \xi_0^2\right) \xi^2 = \epsilon Y_2 \left(\xi_0^1, \xi_0^2\right) \xi^2 \tag{2.44}$$

We solve for the next ξ^1 and ξ^2 until convergence. The smallest eigenvalue and corresponding eigenvector give the ground state energy and the local ground state wave function. The second smallest will bring about the firs excited state energy and the corresponding wave function.

2.4 Summary

From the last tow sections, we see EPT-g1 and EPT-g2 both can solve for the ground state. The EPT-g1 is simpler, but the calculation is heavier because the matrix A for EPT-g1 has larger size than B and D for EPT-g2. However, EPT-g1 is especially suitable for infinit systems with translational symmetry, because only the largest eigenvalue of A needs be retained. On the other hand, EPT-g2 has matrices E and F containing all the eigenvalues and eigenvectors of A, B, C, D, hence it becomes slower than EPT-g1 for infinit systems. Actually we used both EPT-g1 and EPT-g2 (β is set to be 10^{-6} for up to thousand spin sites) for finit spin chains. Since EPT-g2 does not make any approximation and the two methods give exactly the same results and converge with the entanglement at the same speed, the small parameter β in EPT-g1 algorithm is not an issue. Later we will see EPT-g1 calculation for infinit spin 1/2 chains gives very accurate results. Moreover EPT-g's can be applied to the firs excited state for spin 1 chains as well, because the firs excitation occurs when Bloch-Floquet wave number $k = \pi$ which means the bi-site trial wave function structure is suitable to calculate it. On the other hand, the firs excited state in spin 1/2 chains can not be calculated by EPT-g's since it does not have this character. To get the elementary excitation spectrum for spin chains, we have developed a new EPT algorithm, named EPT-e.

CHAPTER 3

EPT FOR THE ELEMENTARY EXCITATION IN ONE DIMENSION

As mentioned in [25], Feynman's effort to explain the roton spectrum (an example of the elementary excitation) is well known[21]. It is important to explain fundamental properties of the superflui ^{4}He [6]. From the Bloch-Floquet theorem, the elementary excitation with wave number k for the Hamiltonian H with translational symmetry is written as

$$\Psi_k = \sum_{m=1}^{L} e^{ikm} \Theta_m^\dagger \mid g\rangle \tag{3.1}$$

EPT for the elementary excitation in one dimension follows this idea. Therefore, L is the total spin site number for spin chains and the summation over m is over the entire spin sites. $\mid g\rangle$ is the ground state. The challenge to use (3.1) to calculate spin chain's excitation spectrum is: first the operator Θ is not determined yet; second, the unrenormalized ground state wave function for an arbitrary spin chain is not easy to get by other existing methods like DMRG. Due to the similar difficultie for many other problems, there is not much progress made along the line of (3.1) since the days of Feynman. Now since EPT-g can precisely calculate the ground state wave function in an unrenormalized form, we can focus only on the firs difficult , i.e., how to determine Θ by EPT algorithm (EPT-e).

EPT-e does this by variating the energy of the excited state, associated with k, with respect to Θ

$$\delta E_k = \delta \frac{\langle \Psi_k \mid H \mid \Psi_k \rangle}{\langle \Psi_k \mid \Psi_k \rangle} = 0 \tag{3.2}$$

Let us write E_k explicitly using (3.1)

$$E_k = \sum_{m,n=1}^{L} e^{-ik(m-n)} \frac{\langle g \mid \Theta_m H \Theta_n^\dagger \mid g \rangle}{\langle \Psi_k \mid \Psi_k \rangle} \tag{3.3}$$

Due to the translational symmetry, $\langle g \mid \Theta_m H \Theta_n^\dagger \mid g \rangle$ is only the function of $m - n$, So (3.3) can be simplifie as

$$E_k = L \sum_{l=1}^{L} e^{-ikl} \frac{\langle g \mid \Theta_l H \Theta_0^\dagger \mid g \rangle}{\langle \Psi_k \mid \Psi_k \rangle} \tag{3.4}$$

Likewise

$$\langle \Psi_k \mid \Psi_k \rangle = L \sum_{l=1}^{L} e^{-ikl} \langle g \mid \Theta_l \Theta_0^\dagger \mid g \rangle \tag{3.5}$$

So the energy gap is

$$\begin{aligned} \epsilon_k = E_k - E_g &= \frac{\sum_{l=1}^{L} e^{-ikl} \langle g \mid \Theta_l (H - E_g) \Theta_0^\dagger \mid g \rangle}{\sum_{l=1}^{L} e^{-ikl} \langle g \mid \Theta_l \Theta_0^\dagger \mid g \rangle} \\ &= \frac{\sum_{l=1}^{L} e^{-ikl} \langle g \mid \Theta_l [H, \Theta_0^\dagger] \mid g \rangle}{\sum_{l=1}^{L} e^{-ikl} \langle g \mid \Theta_l \Theta_0^\dagger \mid g \rangle} \end{aligned} \tag{3.6}$$

where $[\cdots]$ means a commutator. The variation (3.2) is equivalent to $\delta \epsilon_k = 0$ with respect to Θ_l, the cluster operator. We pursue the convergence with respect to the cluster size. In general, for cluster size n the n-cluster operator Θ_l is a linear combination of operator products of n $nd \times nd$ local operators, with $nd = 2$ for spin 1/2 and 3 for spin 1. For spin-triplet exciation, in the simplest case where the size is 1, the cluster operator is uniquely S^+ for spin 1/2, while for spin 1 it could be any linear combination of $= S^+$ and $S^+ S_z$. Now how about the cluster size 2, 3 and so on? Let us take the spin 1/2 chains as example to calculate the rank of the variational space for cluster sizes up to 3. The triplet excitation requires that Θ_l is a linear combination of the 4 local excitation operators for cluster size 2:

$$S^+ \otimes 1 \qquad S^+ \otimes S_z \qquad 1 \otimes S^+ \qquad S_z \otimes S^+$$

It is a linear combination of the 15 local excitation operators for cluster size 3:

$$S^+ \otimes 1 \otimes 1 \qquad S^+ \otimes 1 \otimes S_z \qquad S^+ \otimes S_z \otimes 1 \qquad S^+ \otimes S_z \otimes S_z$$

$$1 \otimes S^+ \otimes 1 \qquad 1 \otimes S^+ \otimes S_z \qquad S_z \otimes S^+ \otimes 1 \qquad S_z \otimes S^+ \otimes S_z$$

$$1 \otimes 1 \otimes S^+ \qquad 1 \otimes S_z \otimes S^+ \qquad S_z \otimes 1 \otimes S^+ \qquad S_z \otimes S_z \otimes S^+$$

$$S^+ \otimes S^+ \otimes S^- \qquad S^+ \otimes S^- \otimes S^+ \qquad S^- \otimes S^+ \otimes S^+$$

Likewise, Θ_l is a linear combination of the 56 local excitation operators for cluster size 4. If we denote the coefficien of these linear combinations by the vector $\tilde{x}$, then the rank of $\tilde{x}$ is 1,4,15 and 56 for cluster sizes 1,2,3 and 4. So (3.2) is reduced to a generalized eigenvalue problem

$$Tx = \epsilon_k U x \tag{3.7}$$

The calculation of T and U is similar to those in EPT-g. It is only a little more lengthy due to the cluster nature and the summation over the entire spin sites. We start with small cluster size, say, 1 and then increase it until convergence. The calculation for spin 1 is the same. Of course the variational space is larger, with the rank of the $\tilde{x}$ being 2,16,126 and 1016 for cluster sizes 1,2,3 and 4.

CHAPTER 4

RESULTS

First we use EPT-g to solve for the ground state properties for both spin 1/2 and 1 chains. EPT-g1 and EPT-g2 gave the same convergence speed. Those properties include ground state energy, local magnetization and spin-spin correlations. We especially investigate the long-range behavior of spin-spin correlations for spin 1/2 chains, considering a very large entanglement and the infinit size. For infinit system EPT-g1 is more suitable as mentioned in Sec.2.4. But for finit systems EPT-g2 works as good as EPT-g1. We also plot the phase diagram for spin 1 xxz chains (below without specifi mentioning, spin chains refer to xxx chains) by using EPT-g to calculate the firs excited state as well as the ground state. Second we use EPT-e to get the spin triplet excitation spectrum for the entire Brillouin zone for both spin 1/2 and spin 1 chains, utilizing the precise ground state wave function obtained by EPT-g. Below we will present the results firs for spin 1/2 and then spin 1. At the last, we show the result of the elementary excitation spectra.

4.1 Spin 1/2 chains

We calculated the spin 1/2 chains with length 16, 32, 64, 128, 256 and 512. The comparison between EPT and Bethe Ansatz[14] for the ground state energies is given in Tab.4.1. Our calculation shows that the necessary entanglement for the convergence to occur increases with the system size. However, Fig.4.1 shows the convergence with entanglement for ground state energy is very quick even for a system as large as 256 sites. We see con-

chain length	EPT result	Bethe Ansatz result
16	-0.4463935	-0.4463935
64	-0.4433459	-0.4433485
256	-0.4431551	-0.4431597

Table 4.1 Comparison of the ground state energies between Bethe Ansatz and EPT

vergence is reached before entanglement $p = 25$. One of the merits of EPT is that it can give precise local wave functions. Hence many quantities can be calculated by using the local wave functions. However, how to judge the local wave function's convergence? We have to fin a quantity by whose convergence with entanglement we can safely say that the local wave function is converged. We found, even though the ground state energy is converged quickly with entanglement, it is not a good candidate. Below we show the results for the local magnetization and spin-spin correlations for a 256-sites chain. Fig.4.2 is the local magnetization. Its convergence can only be achieved after entanglement $p = 30$. Next, we show the spin-spin correlations, $W(l) = \langle S_0^z S_l^z \rangle$, in Fig.4.3. It is shown that the overlapping of $\langle S^z S^z \rangle$ and $\langle S^x S^x \rangle$ curves is a good indicator for the convergence of $W(l)$. Entanglement $p = 35$ gives the convergence. Therefore, the spin-spin correlations ask for the accurate local wave function most strictly, then the local magnetization. Overall, they are the good indicators for accurate local wave functions. Using these indicators we plot the entanglement necessary for convergence versus the system size, as shown in Fig.4.4. Roughly speaking, it is linear for finit size, although we see a little bit bending when L

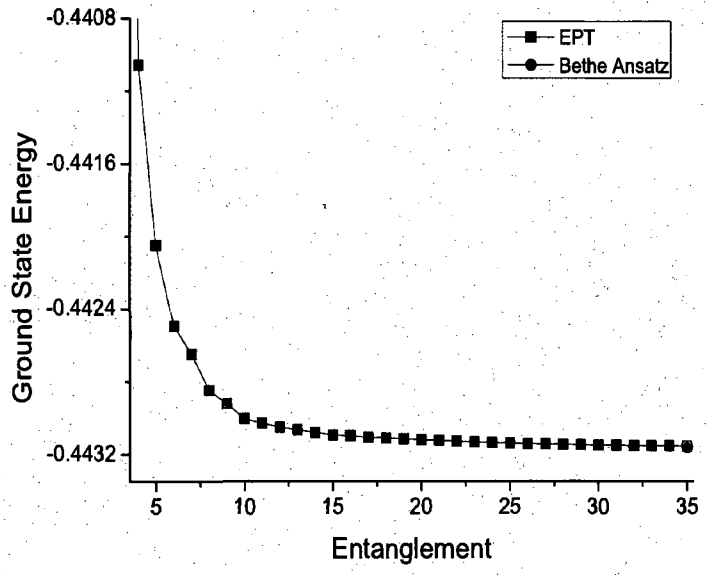

Figure 4.1 Convergence with entanglement of the ground state energy for a 256-sites spin 1/2 chain

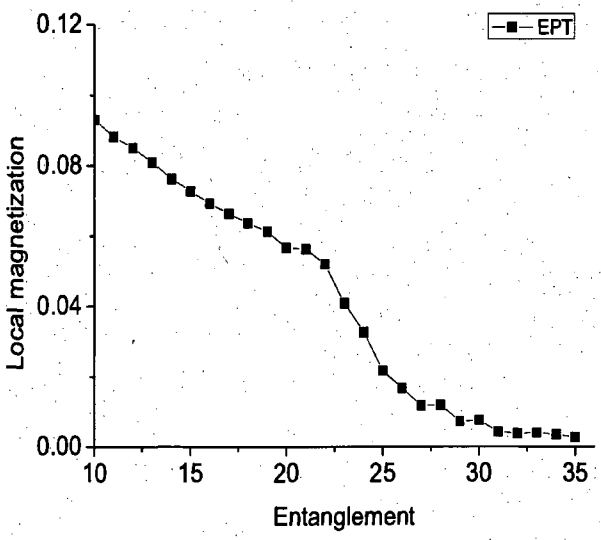

Figure 4.2 Convergence with entanglement of the local magnetization for a 256-sites spin 1/2 chain

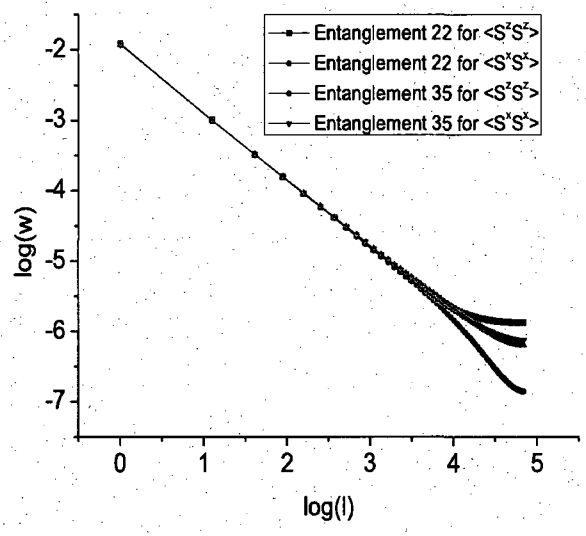

Figure 4.3 Convergence with entanglement of the spin-spin correlations for a 256-sites spin 1/2 chain

becomes larger. This will help us estimate the calculation scale to get a fully converged wave function, namely, all quantities be converged.

The linear fi of the log-log plot of the spin-spin correlations in Fig.4.5 shows a power decay with the exponent of -0.92, conforming there is a a logarithmic factor of $\sqrt{lnl}$ correction to the power decay of l^{-1}[8]. This linear fi is over the firs 101 sites for a 256-sites chain since the curve bends near the center of the chain because of the periodic boundary condition. Fig.4.3 and Fig.4.5 show the unprecedented accuracy of EPT for the long range spin-spin correlations of spin 1/2 chains. To further check its accuracy, we also compare in Tab.4.2 EPT with the Bethe Ansatz (generating function method) [11] for the firs seven sites separations, which is the only rigorous results available by Bethe Ansatz. To compare with conformal fiel theory's prediction of the asymptotic correlation amplitude, a very

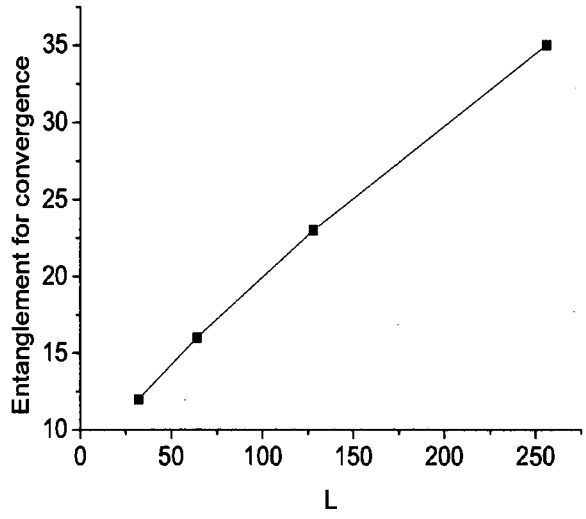

Figure 4.4 The entanglement necessary for convergence versus the system size

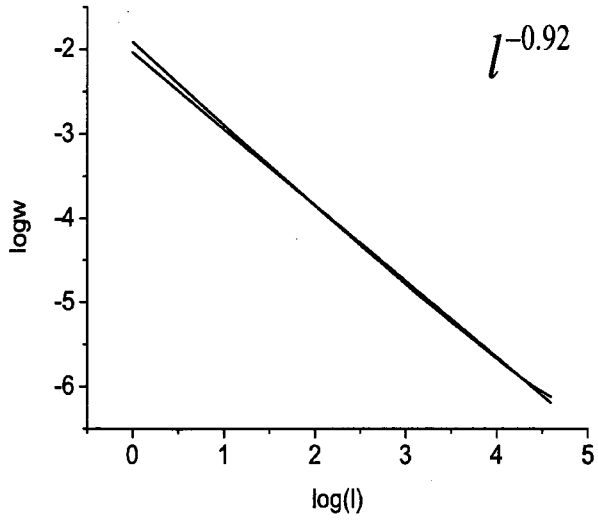

Figure 4.5 Log-log plot of the spin-spin correlation functions over the first 101 sites for a 256-sites spin 1/2 chain

distance	EPT	Bethe Ansatz
1	-0.1477158	-0.1477157
2	0.0606715	0.0606798
3	-0.0502196	-0.0502486
4	0.0346027	0.0346528
5	-0.0308457	-0.0308904
6	0.0243621	0.0244467
7	-0.0223980	-0.0224982

Table 4.2 Comparison between EPT and Bethe Ansatz over the first seven sites

long spin chain has to be calculated. So we have calculated the infinit spin 1/2 chain by EPT-g1. Due to the limitation of the available computing resources, currently we only calculated for entanglement up to 85. With such a large entanglement, the ground state energy is very accurate, -0.4431463 versus -1.4431471 from Bethe Ansatz. However, $\langle S^z S^z \rangle$ and $\langle S^x S^x \rangle$ curves do not overlap for the entire range of the firs 1500 site separations, only at which the accuracy of field-theor prediction seems be checked. Comparing with the $p = 50$ result, Fig.4.6, indicates a tendency to the convergence around $p = 120$. We will keep working on this.

4.2 Spin 1 chains

Similarly we calculated the spin 1 chains with many different lengths. We compare the EPT results with DMRG calculation[29]. For example, the ground state energy for a 48 site

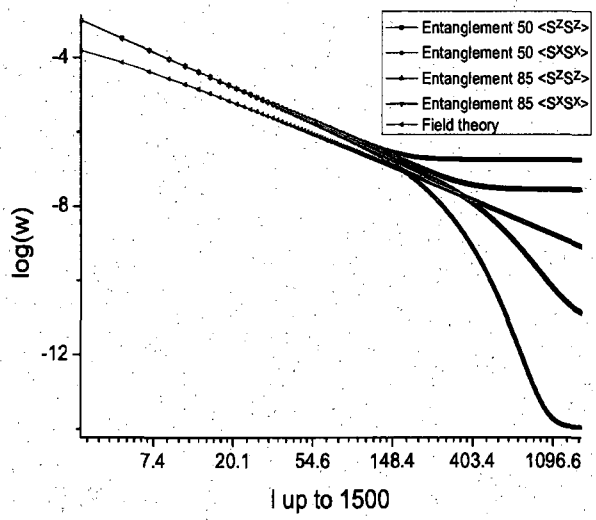

Figure 4.6 Spin-spin correlation functions for an infinite spin 1/2 chain

chain is -1.401482 by EPT versus -1.401484 by DMRG[29]. The energy gap between the ground state energy and the firs excited state energy for the same chain is 0.41242 by EPT and 0.41232 by DMRG. Using the calculated ground sate wave function, we calculated the spin-spin correlations. We see a clear convergence of the semi-log curve of the correlation functions at entanglement $p = 18$ for a 64-site chain in Fig.4.7. The straight line in semi-log plot indicates an exponential decay of the spin-spin correlation with the distance, consistant with the existence of the energy gap in spin 1 chains. Using EPT-g to calculate spin 1 xxz chains is especially handy. One only needs slightly vary the operator Γ^1 and Γ^2 in (2.15) to include the anisotropic spin z-component coupling, $\lambda \neq 1$. Below we show its phase diagram In Fig.4.8, the four phases are precisely identified When λ decreases from a fairly large value, the spin 1 xxz chains enter from Neel phase to Haldane phase. At $\lambda = 1.192$,

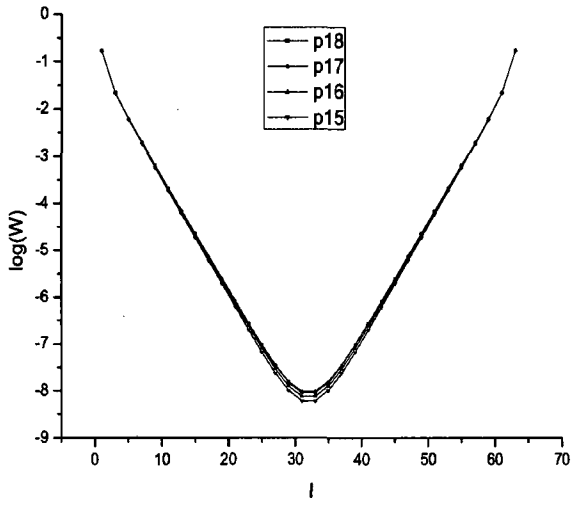

Figure 4.7 The spin-spin correlation functions exponentially decay with the distance

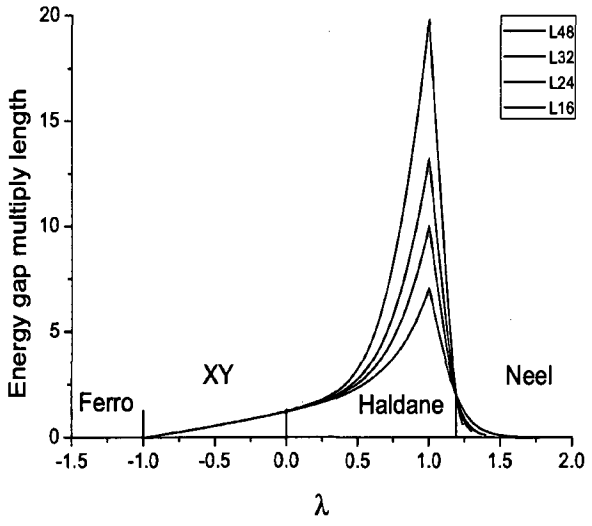

Figure 4.8 Phase diagram for spin 1 xxz chains

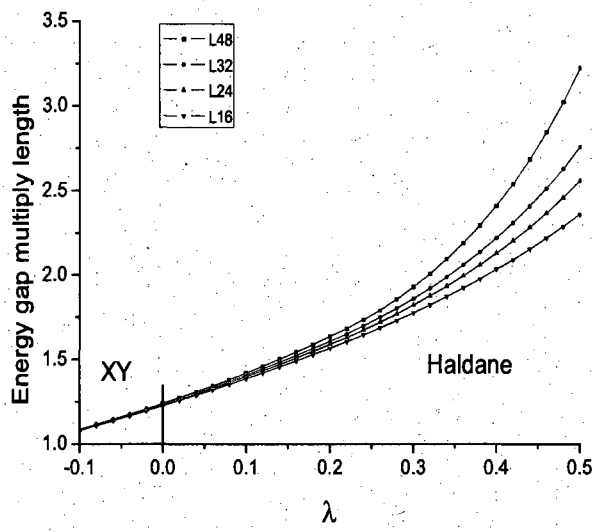

Figure 4.9 Amplified region where the transition from Haldane phase to XY phase occurs

the energy gap for an infinit chain disappears. From this point to $\lambda = 0$ there is energy gap for all chain length. And at $\lambda = 1$, the energy gap converged to a finit value. See Fig.4.10 From $\lambda = 0$ to $\lambda = -1$ is the XY phase, the infinit spin chain has no energy gap. At $\lambda = -1$, every finit chains have no energy gap. After this point, it enters ferromagnetic phase, where the ground state is doublly degenerate. Fig.4.9 shows that the EPT calculation precisely captured the transition point between the XY phase and the Haldane phase. The phase diagram by EPT agrees with the fiel theory [31].

4.3 Spin triplet excitation spectra

We use EPT-e to calculate the spin triplet excitation spectrum for spin 1/2 with the chain size 512 and the cluster size n up to 4. From top to bottom the cluster size varies from 1 to 4. In Fig.4.11 we see the agreement is within 1% with the solid line from Bethe Ansatz

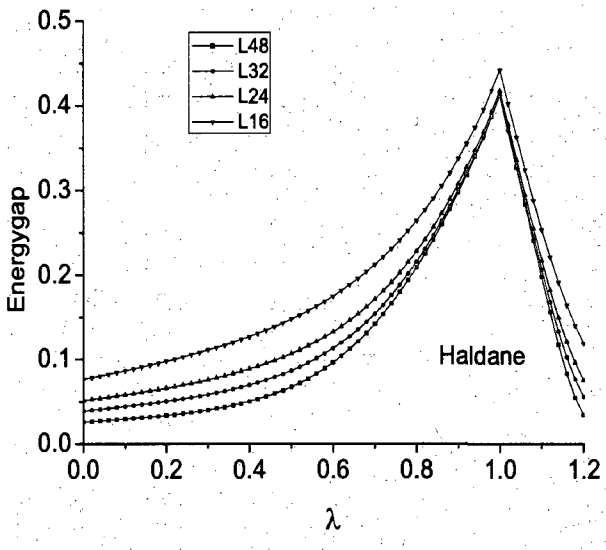

Figure 4.10 Haldane gap at $\lambda = 1.0$ for spin 1 chains

[2]. Considering that this calculation used the ground state by EPT-g with entanglement $p = 20$, the discrepancy might have two possible sources. One is that the ground state with $p = 20$ for 512 sites contains a tiny error. Another is that the ultimate result might still gain small contribution after n increases beyond 4. Pursuing the ground state with larger entanglement may improve the result to certain extent without too much effort. Beyond that we have to use $n = 5$ or so. We see more clearly the role which n and p play in Fig.4.12 for the spin 1 chain, where from top to bottom n varies from 1 to 3, while $p = 24$. We see that although $n = 3$ result is not quite converged, from $n = 2$ to $n = 3$ the precision improves more in spin 1 calculation than in spin 1/2 case. It is the larger entanglement that gives more accurate ground state which makes this difference. Let us discuss the spin triplet spectrum for spin 1 in more details. The Haldane gap at $k = \pi$ is found by EPT to be 0.414

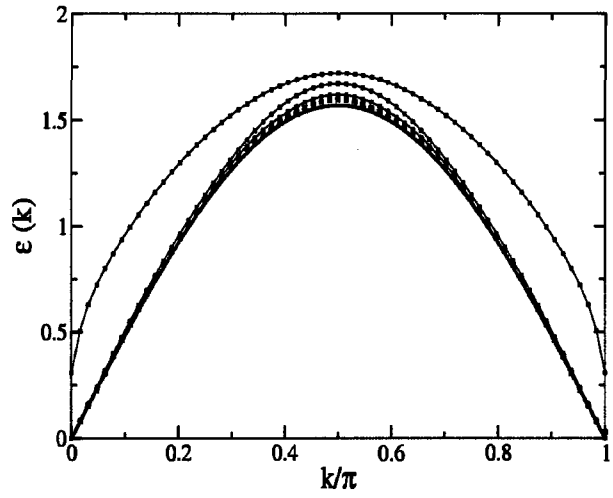

Figure 4.11 Spin triplet excitation spectrum for a 512-sites spin 1/2 chain

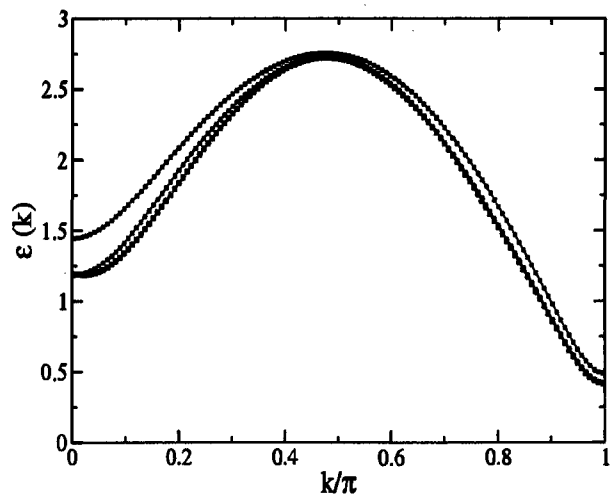

Figure 4.12 Spin triplet excitation spectrum for 512-sites spin 1 chain

agreeing with the other methods[17, 29, 11]. The spectrum in the region $0 \leq k/\pi \leq 1/2$ is believed to be embedded in a continuum spectrum of a pair of magnons with the total spin z-component to be 0[1]. Takahashi [18] used the exact diagonalization method to calculate the excitation spectra for a 20-site chain, showing that the lowest excitation at $k = 0$ is indeed a spin singlet, presumably a pair of spin triplet magnons from $k = \pm\pi$[9, 11]. However the system size that the diagonalization method can handle is rather limited since the size of the matrix to be diagonalized increases very quickly. We believe that the spin triplet magnon spectrum for spin 1 for the entire Brillouin zone has been determined for the firs time by EPT. Moreover, EPT can handle other excitations such as spin-singlet, if we calculate not only the minimum but all the eigenvalues of (3.7). Such entire excitation spectra have been solved by Bethe Ansatz [1] only for the isotropic spin 1/2 chain.

CHAPTER 5

CONCLUSION

Two EPT algorithms, EPT-g1 and EPT-g2, have been applied to solve for the ground sate properties for antiferromagnetic spin chains. EPT-g can also calculate the firs excitated state for spin 1, which enabled us to determine the phase diagram of the spin 1 xxz chains. During the calculations, we found EPT has a high efficien y for finit spin chains, namely fast convergence with entanglement. Although the current calculation is not sufficien to directly check the singular behavior of an infint spin 1/2 chain for $\langle S_0^z S_l^z \rangle$ and $\langle S_0^x S_l^x \rangle$ predicted by the fiel theory [8, 16], when λ varies from 1^- to 1 or from $1^+$to 1, we did see a tendency. But a further investigation is needed. On the other hand, using the ground state by EPT-g, the EPT algorithm for elementary excitation in one dimention determined the spin triplet excitation spetra for both spin 1/2 and spin 1. In particular the spin-triplet magnon spectrum for spin 1 chain for the entire Brillouin zone has been determined by EPT for the firs time, including the Haldane gap at $k = \pi$

EPT agrees with Bethe Ansatz for the ground state properties of spin 1/2 chains. Bethe Ansatz is rigorous, it precisely calculates some quantities, such as the ground state and low lying excited states. However, rigorously calculable quantities are limited. For example, the spin-spin correlation functions are calculated by Bethe Ansatz only for a short-distance separation. EPT also agrees with DMRG concerning the ground state energy and Haldane gap in spin 1 chains. While DMRG has seen a remarkable success in various condensed matter systems, its application to two space dimensions has been limited, most likely re-

vealing the failure of the very idea of the Hilbert space truncation. As for other methods, their application is either limited or they can only calculate specifi quantities, such as conformal fiel theory [8, 27] gives the asympotic correlation amplitude. On the other hand, EPT systematically solves the spin chains in that it precisely solves the local wave functions with high efficien y in an unrenormalized form. Once one has the wave functions, many other properties can be readily obtained.

The spin chain study here along with the previous study of 2D&3D Ising models, 1D&2D Hubbard models and the recently started Bose-Hurbard model, show that EPT is a general method for strongly correlated quantum systems with translational symmetry. Moreover, EPT-e's success also indicates that EPT can handle imhomorgeneous systems like nano-structures embedded in correlated host materials.

BIBLIOGRAPHY

1. B.J.STERNLIEB, S. C. D., AND R.W.ERWIN. Dominance of long-lived excitations in the antiferromagnetic spin-1 chain nenp. *Phys. Rev. Lett. 33* (1986), 659.

2. CLOISEAUX, J., AND J.J.PEARSON. Spin-wave spectrum of the antiferromagnetic linear chain. *Phys. Rev. 128* (1962), 2131.

3. C.N.YANG, AND C.P.YANG. One-dimensional chain of anisotropic spin-spin interactions. i. proof of bethe's hypothesis for ground state in a finit system. *Phys. Rev 150* (1966), 321.

4. C.N.YANG, AND C.P.YANG. One-dimensional chain of anisotropic spin-spin interactions. ii. properties of the ground-state energy per lattice site for an infinit system. *Phys. Rev 150* (1966), 327.

5. C.N.YANG, AND C.P.YANG. One-dimensional chain of anisotropic spin-spin interactions. iii. applications. *Phys. Rev 151* (1966), 258.

6. D.R.TILLEY, AND J.TILLEY. Superfluidit and Superconductivity (Adam Hilger LTD, Bristol, 1986).

7. F.D.M.HALDANE. Nonlinear fiel theory of large-spin heisenberg antiferromagnets: Semiclassically quantized solitons of the one-dimensional easy-axis néel state. *Phys. Rev. Lett. 50* (19837), 1153.

8. I.AFFECK. Exact correlation amplitude for the s=1/2 heisenberg antiferromagnetic chain. *J.Phys. A:Math. Gen 31* (1998), 4573.

9. J.B.PARKINGSON, AND J.C.BONNER. Spin chains in a field Crossover from quantum to classical behaivior. *Phys. Rev. B 32* (1985), 4703.

10. J.LINKS, A.FOERSTER, AND M.KAROWSKI. Bethe ansatz solution of a closed spin 1 xxz heisenberg chain with quantum algebra symmetry. *J. Math. Phys. 40* (1999), 726.

11. J.SATO, M., AND M.TAKAHASHI. Correlation functions of the spn-1/2 antiferromagnetic heisenberg chain: Exact calculation via the generating function. *J.Phys. A:Math. Gen 729* (2005), 441.

12. LIANG, S. Monte carlo calculations of the correlation functions for heisenberg spin chains at t=0. *Phys. Rev. Lett. 64* (1990), 1597.

13. M.KARBACH, AND G.MULLER. cond-mat/9809162 v1 10sep 1998.

14. M.KARBACH, K.HU, AND G.MULLER. cond-mat/9809163 v1 10sep 1998.

15. M.KARBACH, K.HU, AND G.MULLER. cond-mat/0008018 v1 1Aug 2000.

16. M.P.A. FISHER, P.B. WEICHMAN, G., AND FISHER, D. Boson localization and the superfluid-insulato transition. *Phys. Rev. B 40* (1989), 546.

17. M.P.NIGHTINGALE, AND H.W.J.BLOTE. Gap of the linear spin-1 heisenberg antiferromagnet: A monte carlo calculation. *Phys. Rev. B 33* (1986), 659.

18. M.TAKAHASHI. Excitatin spectra of s=1 antiferromagnetic chains. *Phys. Rev. B 50* (1994), 3045.

19. P.SCHLOTTMANN. Heisenberg spin chain with many impurities. *Phys. Rev. B 49* (1994), 9202.

20. P.W.ANDERSON. An approximate quantum theory of the antiferromagnetic ground state. *Phys. Rev. 86* (1952), 694.

21. R.P.FEYNMAN. Atomic theory of the two-flui model of liquid helium. *Phys. Rev. 94* (1954), 262.

22. S.G.CHUNG. New method for the 3d ising model. *Phys. Lett. A 359* (2006), 707.

23. S.G.CHUNG. New method for the quantum ground states in one dimesion. *Phys. Lett. A 361* (2006), 396.

24. S.G.CHUNG, AND K.UEDA. Entanglement perturbation theory for the quantum ground states in two dimensions. *Phys. Lett. A 372* (2008), 4845.

25. S.G.CHUNG, AND WANG, L. Entanglement perturbation theory for the elementary excitation in one dimension, Phys. Lett. A, in press.

26. S.K.PATI, S.RAMASESHA, AND D.SEN. Low-lying excited states and low-temperature properties of an alternating spin-1-spin-1/2 chain: A density-matrix renormalization-group study. *Phys. Rev. B 55* (1997), 8894.

27. S.LUKYANOV, AND TERRAS, V. Long-distance asymptotics of spin-spin correlation functions for the xxz spin chain. *Nuclear Physics B 654* (2003), 323.

28. S.R.WHITE. Density-matrix algorithms for quantum renormalization groups. *Phys. Rev.B 48* (1993), 10345.

29. S.R.WHITE, AND D.A.HUSE. Numerical renormalization-group study of low-lying eigenstates of the antiferromagnetic s=1 heisenberg chain. *Phys. Rev.B 48* (1993), 3844.

30. T.HIKIHARA, AND A.FURUSAKI. Correlation amplitudes for the spin-1/2 xxz chain in a magnetic field *Phys. Rev. B 69* (2004), 064427.

31. W. CHEN, K. H., AND SANCTUARY, B. Ground-state phase diagram of s=1 xxz chains with uniaxial single-ion-type anisotropy. *Phys. Rev. B 67* (2003), 104401.